Supplement of Atmos. Chem. Phys., 20, 8533–8549, 2020
https://doi.org/10.5194/acp-20-8533-2020-supplement

Atmospheric Chemistry and Physics
Open Access
EGU

Supplement of

Particle number concentrations and size distribution in a polluted megacity: the Delhi Aerosol Supersite study

Shahzad Gani et al.

Correspondence to: Joshua S. Apte (jsapte@utexas.edu) and Lea Hildebrandt Ruiz (lhr@che.utexas.edu)

Table S1. Seasonal summary of PN species—arithmetic mean (AM), geometric mean (GM), and geometric standard deviation (GSD) for hourly concentrations.

	AM ($\times 10^3$ cm^{-3})					GM ($\times 10^3$ cm^{-3}) (GSD)				
	Winter	Spring	Summer	Monsoon	Autumn	Winter	Spring	Summer	Monsoon	Autumn
N_{nuc}[a]	6.3	12.4	10.6	10.3	5.0	4.0 (2.9)	9.1 (2.4)	7.5 (2.4)	6.4 (2.8)	3.0 (2.9)
N_{ait}[a]	26.4	23.5	21.9	17.8	19.1	21.7 (1.9)	20.6 (1.7)	18.4 (1.8)	15.2 (1.8)	15.9 (1.9)
N_{acc}[a]	18.2	11.7	9.7	6.3	12.9	15.3 (1.8)	9.8 (1.8)	7.7 (2.0)	5.2 (1.9)	10.5 (2.1)
UFP[b]	32.7	35.9	32.5	28.1	24.1	28.5 (1.8)	32.8 (1.6)	28.3 (1.8)	23.9 (1.9)	20.6 (1.9)
PN[c]	50.9	47.6	42.2	34.4	37.0	46.2 (1.7)	45.0 (1.5)	38.3 (1.7)	30.8 (1.7)	33.2 (1.8)

[a]The modes are based on SMPS observations—nucleation ($12 < D_p < 25$ nm), Aitken ($25 < D_p < 100$ nm) and accumulation ($100 < D_p < 560$ nm) modes. [b]UFP = N_{nuc} + N_{ait}. [c]PN = UFP + N_{acc}.

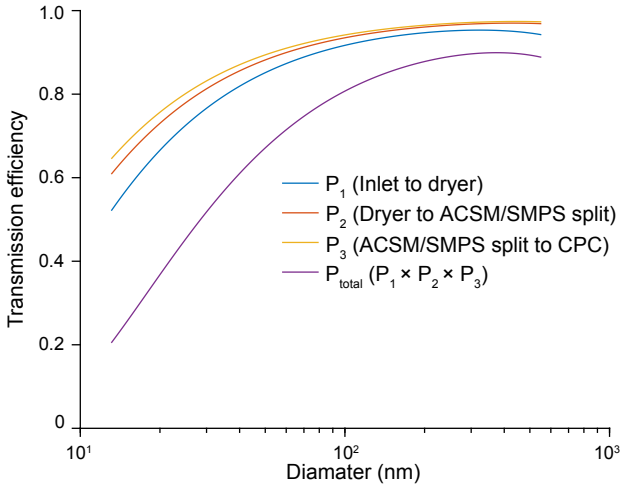

Figure S1. Transmission efficiency for the DAS sampling line calculated for diffusion (Ingham, 1975) and settling (Pich, 1972) losses.

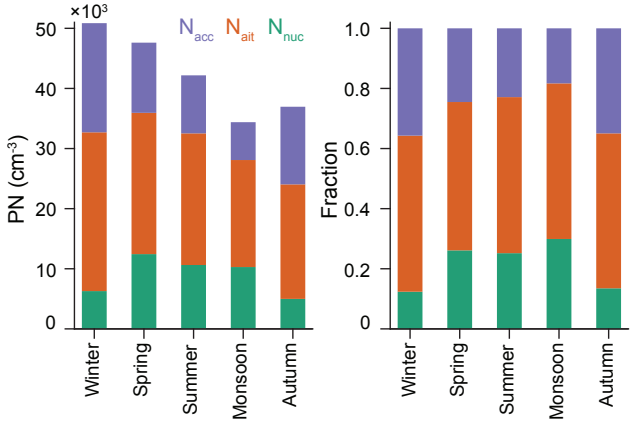

Figure S2. Average absolute and fractional PN levels for each season by mode. The modes are based on SMPS observations—nucleation ($12 < D_p < 25$ nm), Aitken ($25 < D_p < 100$ nm) and accumulation ($100 < D_p < 560$ nm) modes.

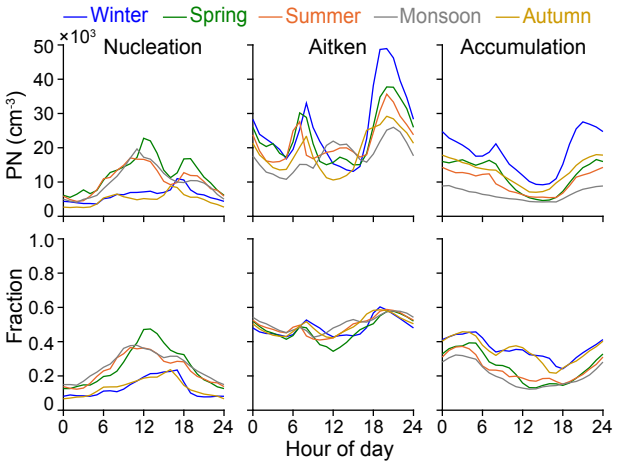

Figure S3. Average absolute and fractional modes of PN (nucleation (D_p < 25 nm), Aitken (25 < D_p < 100 nm) and accumulation (D_p > 100 nm)) by season and time of day.

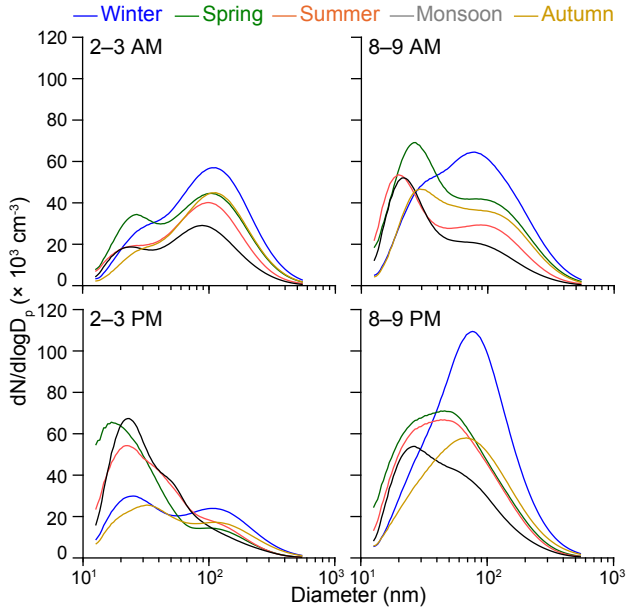

Figure S4. Particle size distribution for particles between 12–560 nm. Four indicative time periods are presented; 8–9 AM for morning rush hour, 2–3 PM for midday (high dilution), 8–9 PM for evening rush hour and 2–3 PM for late night (low dilution and low emissions).

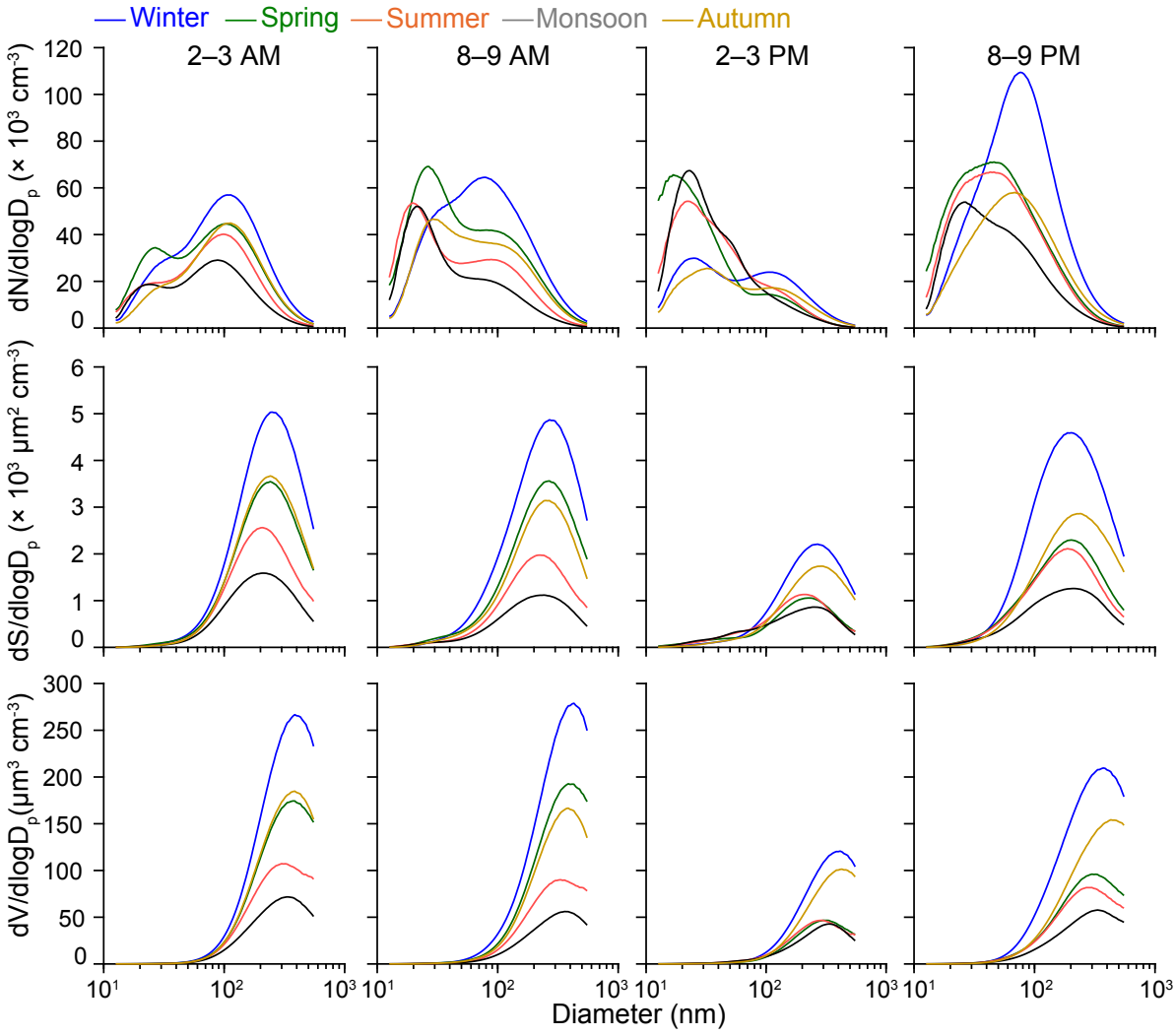

Figure S5. Number, surface area and volume concentrations for particles between 12–560 nm. Four indicative time periods are presented; 8–9 AM for morning rush hour, 2–3 PM for midday (high dilution), 8–9 PM for evening rush hour and 2–3 PM for late night (low dilution and low emissions).

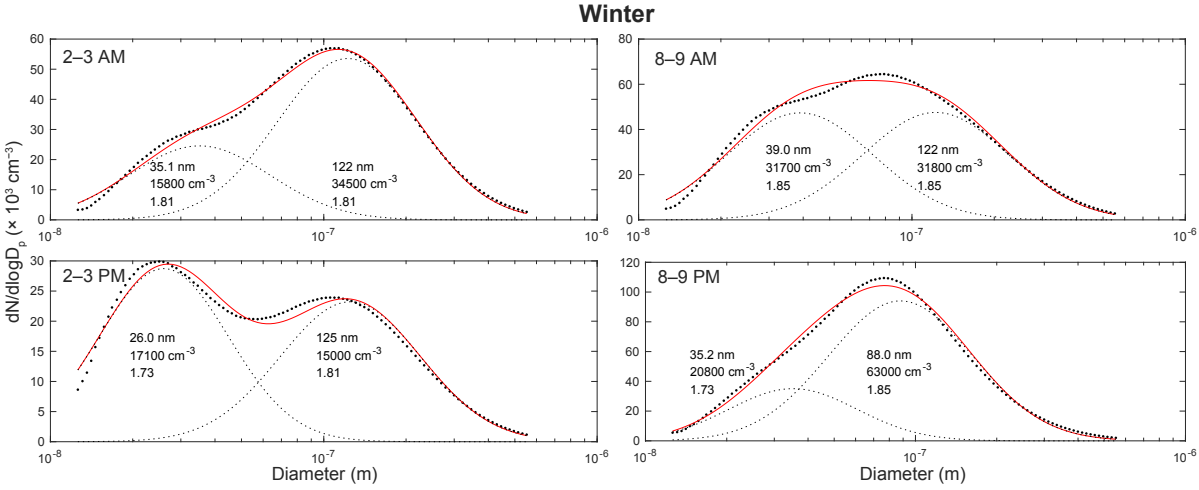

Figure S6. Multi-lognormal fit for PSD averaged over winter.

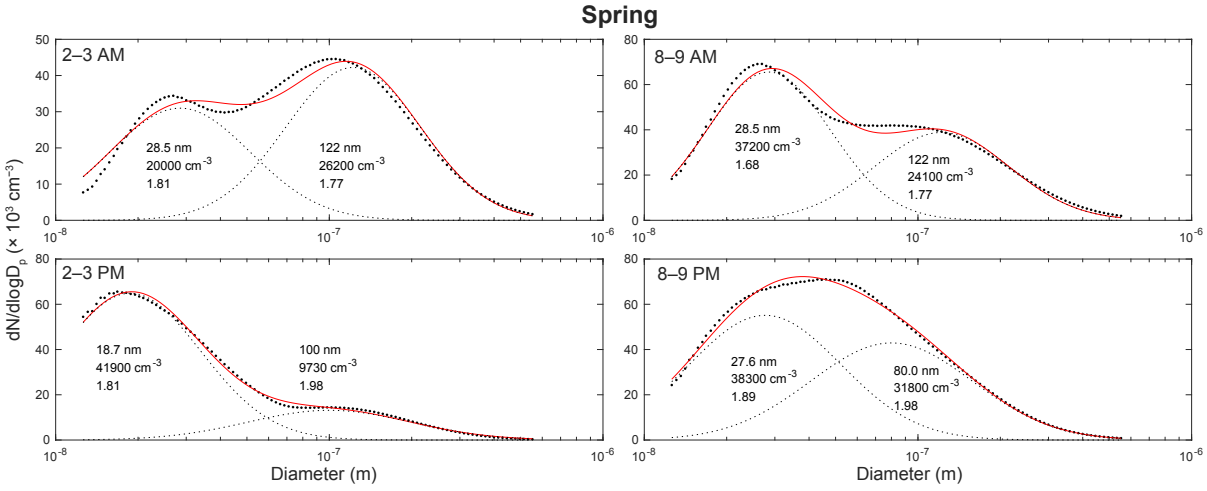

Figure S7. Multi-lognormal fit for PSD averaged over spring.

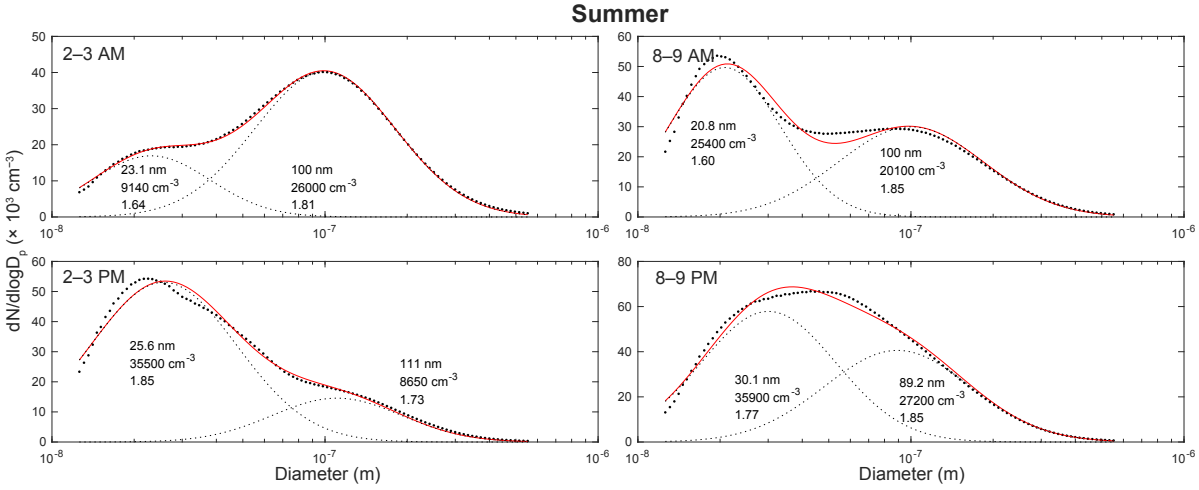

Figure S8. Multi-lognormal fit for PSD averaged over summer.

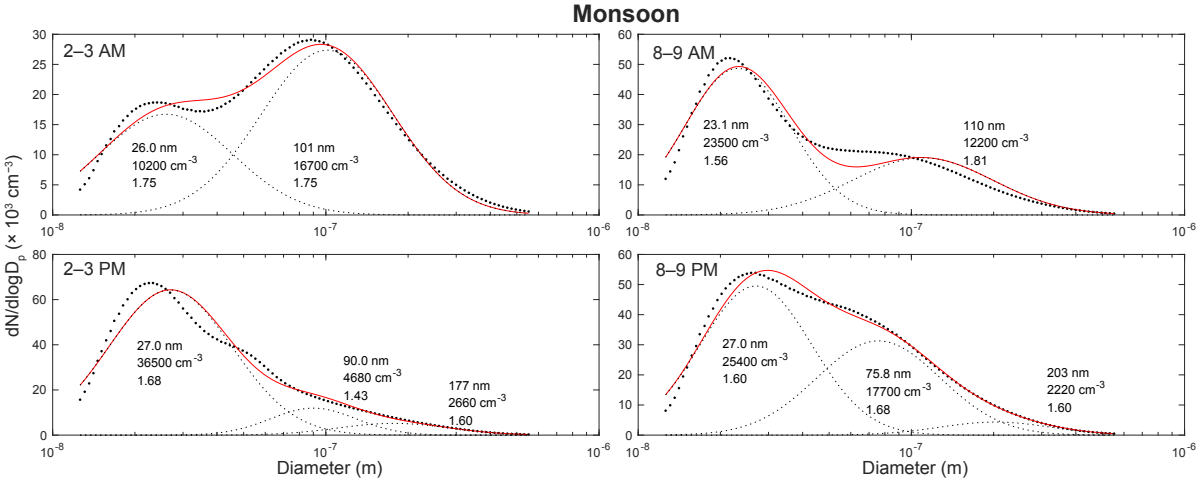

Figure S9. Multi-lognormal fit for PSD averaged over monsoon.

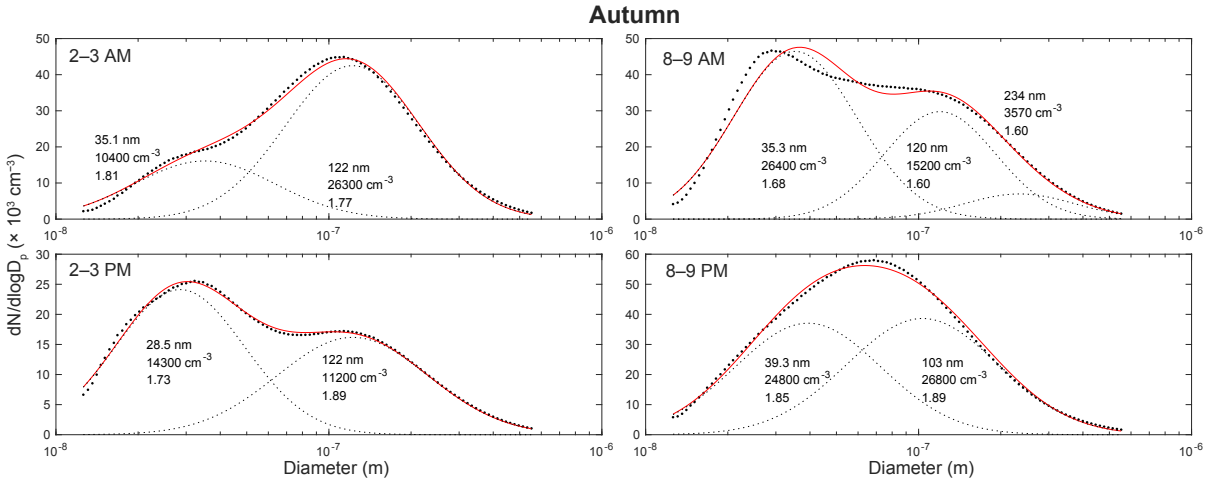

Figure S10. Multi-lognormal fit for PSD averaged over autumn.

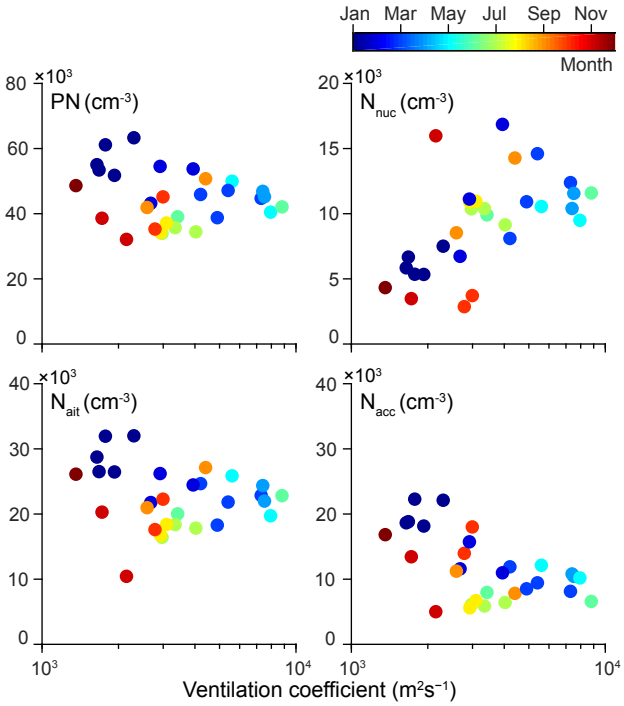

Figure S11. Variations of number concentrations as a function of ventilation coefficient for PN, N_{nuc} ($D_p < 25$ nm), N_{ait} ($25 < D_p < 100$ nm), and N_{acc} ($D_p > 100$ nm). Each scatter point is a two-week average and is color-coded with the month. Note that July to mid-September is the monsoon season.

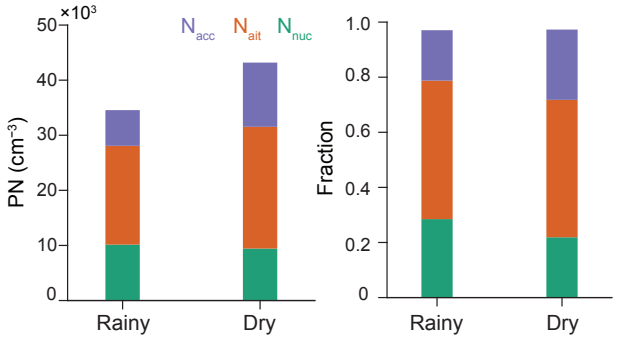

Figure S12. Average PN concentrations for days with (rainy) and without rain (dry) during the monsoon season.

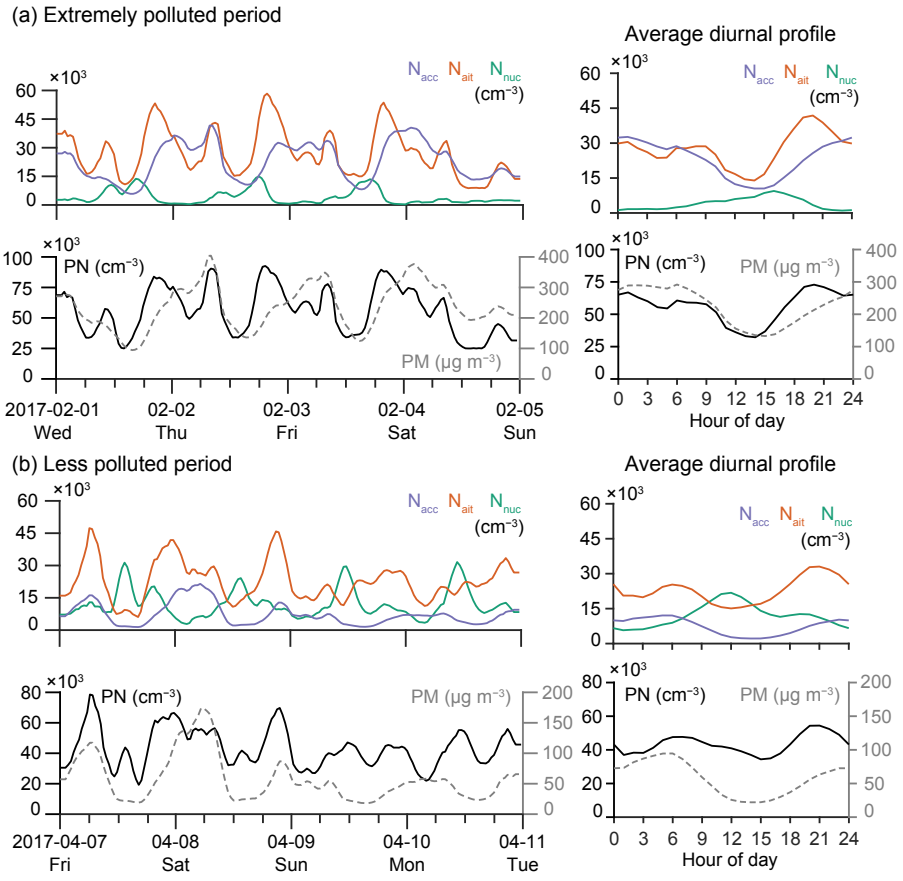

Figure S13. Timeseries for a (a) polluted period with prominent coagulation scavenging and (b) less polluted period with some new particle formation and growth. N_{nuc} ($D_p < 25$ nm), N_{ait} ($25 < D_p < 100$ nm), and N_{acc} ($D_p > 100$ nm) concentrations are presented for both periods. The average diurnal profile of the the three size modes along with the PN and PM concentrations over the two periods are presented in the right panels. Estimation of PM concentrations were based on the volume concentrations observed by the SMPS and assuming particle density to be 1.6 g cm^{-3}.

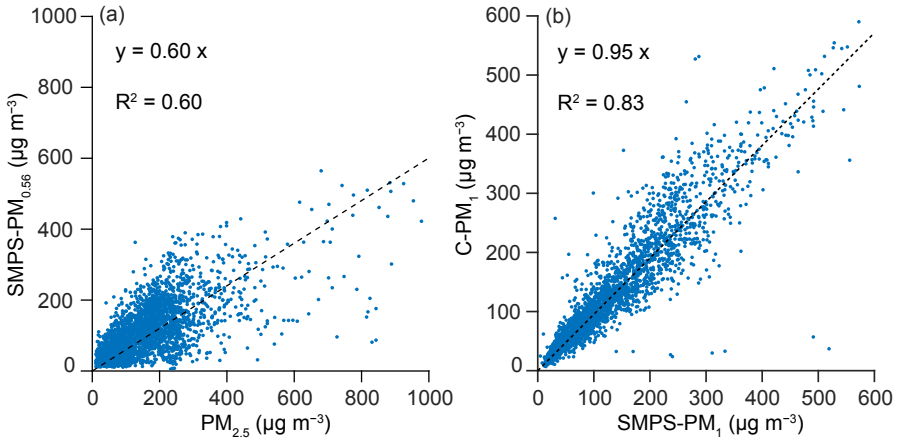

Figure S14. Scatter plot between (a) SMPS-$PM_{0.56}$ and $PM_{2.5}$ (b) C-PM_1 (Composition-PM_1 = NR-PM_1 + BC) and SMPS-PM_1. SMPS-PM estimated using PSD and assuming a density of 1.6 g cm^{-3}). $PM_{2.5}$ concentration data from a regulatory monitor (DPCC, R.K. Puram, 3 km from our site). Subplot (b) was reproduced from the supplement of Gani et al. (2019).

References

Gani, S., Bhandari, S., Seraj, S., Wang, D. S., Patel, K., Soni, P., Arub, Z., Habib, G., Hildebrandt Ruiz, L., and Apte, J. S.: Submicron aerosol composition in the world's most polluted megacity: the Delhi Aerosol Supersite study, Atmospheric Chemistry and Physics, 19, 6843–6859, https://doi.org/10.5194/acp-19-6843-2019, 2019.

Ingham, D.: Diffusion of aerosols from a stream flowing through a cylindrical tube, Journal of Aerosol Science, 6, 125–132, https://doi.org/10.1016/0021-8502(75)90005-1, 1975.

Pich, J.: Theory of gravitational deposition of particles from laminar flows in channels, Journal of Aerosol Science, 3, 351–361, https://doi.org/10.1016/0021-8502(72)90090-0, 1972.